Adsorption (2023) 29:163–176
https://doi.org/10.1007/s10450-023-00384-0

Adsorption of bovine serum albumin on a mixed-mode resin - influence of salts and the pH value

Jannette Kreusser[1] · Hans Hasse[1] · Fabian Jirasek[1]

Received: 23 April 2022 / Revised: 4 April 2023 / Accepted: 11 April 2023 / Published online: 7 May 2023

Abstract
The separation and purification of proteins is often carried out by chromatography. Mixed-mode adsorbents are interesting as they may combine favorable features of different chromatographic methods, such as ion-exchange chromatography (IEC) and hydrophobic interaction chromatography (HIC). Systematic experimental studies and models of adsorption isotherms of proteins on mixed-mode resins covering a wide range of parameters are still rare, which hampers both the scientific analysis of the complex processes that occur upon the adsorption of proteins on these resins as well as the practical separation design. Therefore, such studies were carried out in the present work for a model system: the adsorption of bovine serum albumin (BSA) on the mixed-mode resin Toyopearl MX-Trp-650M, which combines features of IEC and HIC resins. Adsorption isotherms were measured using sodium chloride, sodium sulfate, ammonium chloride, and ammonium sulfate at ionic strengths up to 3000 mM and for pH 4.0, 4.7, and 7.0 at 25 °C. In the studied pH ranges, BSA exhibits strongly varying net charges and undergoes a conformational change. At pH 4.0 and 4.7, an exponential decay of the BSA adsorption with increasing ionic strength was found at ionic strengths up to approximately 1000 mM, while a rather linear increase was observed at higher ionic strengths for all studied salts; for all salts and ionic strengths, decreasing adsorption with increasing pH value was found. Moreover, a mathematical model was developed, which enables the prediction of equilibrium adsorption isotherms of BSA on Toyopearl MX-Trp-650M for any ionic strength of the studied salts.

Keywords Chromatography · Proteins · Ionic strength · Adsorption isotherms · Modeling

1 Introduction

Mixed-mode chromatography (MMC) is an attractive chromatographic method, in particular for challenging protein separation and purification processes [1, 2]. The combination of ligands with different interaction mechanisms on mixed-mode resins, most commonly ligands used in ion exchange chromatography (IEC) and ones used in hydrophobic interaction chromatography (HIC), may offer advantages compared to traditional single-mode resins; when we talk about mixed-mode resins in the following, we always refer to this combination of types of ligands. For instance, mixed-mode resins usually provide higher protein loading capacities compared to HIC resins [3], in particular at low ionic strengths, where protein adsorption is dominated by ionic interactions [4, 5]. IEC resins, on the other hand, usually have low binding capacities at high ionic strengths due to shielding effects of the ions present in solution. In contrast, MMC resins exhibit a higher salt tolerance and therefore wider operating ranges [1, 6], since protein adsorption is facilitated at high ionic strengths by hydrophobic interactions on the HIC part of the mixed-mode resin. Furthermore, different interaction modes in MMC enable separations even of very similar proteins [7, 8], e.g., conjugates.

Protein adsorption is a complex process and many parameters, such as the presence of salts in solution, pH value, and temperature, need to be considered for understanding and describing the process, even if only single-mode resins are considered; the situation becomes more complicated if mixed-mode resins are studied. For instance, the addition of

✉ Fabian Jirasek
fabian.jirasek@mv.uni-kl.de

Jannette Kreusser
jannette.kreusser@mv.uni-kl.de

Hans Hasse
hans.hasse@mv.uni-kl.de

[1] Laboratory of Engineering Thermodynamics (LTD), TU Kaiserslautern, Erwin-Schrödinger-Straße 44, 67663 Kaiserslautern, Germany

salts to the mobile phase can have opposing effects on the adsorption equilibrium in MMC. On the one hand, ions in solution shield electric charges on the surface of the protein molecules and of the ionic ligands [9], which leads to lower protein adsorption on the IEC sites of the resin with increasing ionic strength. On the other hand, ions interact with the water molecules in solution, which, depending on the type of ions, may result in a weakening of the proteins' hydrate shells [10]; the resulting salting-out effect leads to favored hydrophobic interactions between the protein molecules and the HIC ligands of the mixed-mode resin [11] and therefore to an increased adsorption with increasing ionic strength.

The adsorption in MMC is also strongly influenced by the pH value. IEC adsorption is based on the attraction of opposite surface charges of resin and protein [12], which in turn depend on the pH value via the dissociation equilibria of the proteins and the ligands. There are two points of zero charge: the isoionic point (IIP), for which exclusively the zwitterion is regarded, and the isoelectric point (IEP), for which also the ions that are strongly bound to the surface charges of the zwitterion and therefore are arranged closely around the zwitterion are considered [13]. Both points are dependent on the ionic strength: the IIP of bovine serum albumin (BSA) has been observed to increase with increasing ionic strength, while the IEP of BSA decreases with increasing ionic strength [13]. In the following, only the IEP of BSA is considered since, from a technical point of view, also the influence of ions closely surrounding the BSA molecules should be taken into account for describing the adsorption of BSA. At pH values below the IEP of the protein, the protein's net charge is positive, while it is negative for pH values above the IEP [14, 15]. The protein's net charge, and hence the pH value, have a significant impact on the adsorption mechanisms of the mixed-mode resin: larger *opposing* net charges of protein and IEC ligands lead to stronger *attractive* ionic interactions on the IEC part of the resin, whereas large absolute net charges of the protein in general hamper a closer packing of protein molecules due to electrostatic repulsion [11].

Moreover, not only the proteins' net charge, but also the proteins' conformation can change as a function of the pH value. BSA is a prominent example for such a protein as it undergoes several confirmation changes with varying pH value. In total five isomers of BSA are known: at pH values around its IEP (at approximately pH 4.7 [16], which, however, can vary slightly with varying ionic strength [13]), BSA is present in the so-called "normal" (N) conformation, also called "heart-shaped" conformation, in solution [17]. Below pH 4.0, the so-called "fast migrating" (F) shape, also called "cigar-shaped" conformation, occurs, which transitions to the denatured "expanded" (E) conformation at very low pH values [17]. Above pH 8.0, the so-called "basic" (B) shape is found, which transitions to the "aged" (A) conformation at even higher pH values [17]. The conformation in which BSA is present in solution significantly influences both the size and the nature of the protein's surface area that is accessible for adsorption; for instance, the expanded F-BSA exhibits a larger hydrophobic surface area than the more globular N-BSA [18].

Systematic experimental studies of the adsorption of proteins on mixed-mode resins that cover broad value ranges of the multiple parameters that are important for the adsorption process are still lacking to date. The comparatively few available experimental studies on adsorption isotherms of proteins on MMC resins are mainly restricted to solutions containing sodium chloride and low ionic strengths, e.g., [19–22]; [23, 24] additionally consider solutions containing ammonium sulfate for ionic strengths up to 1500 mM. As a consequence, also suitable models for comprehensively describing the adsorption of proteins on mixed-mode resins are not available at present; the few existing modeling approaches, e.g., [4, 25, 26], are limited to solutions containing sodium chloride.

To close this gap, we have recently developed a model for describing the adsorption of the model protein lysozyme on Toyopearl-Mx-Trp-650M for four salts (sodium chloride, sodium sulfate, ammonium chloride, and ammonium sulfate) at ionic strengths up to 3000 mM and pH values between 5.0 and 8.0 [27, 28]. It is based on an approach from earlier work of our group for modeling adsorption equilibria in HIC [29–33] and does not only reproduce the adsorption data for a wide range of the studied conditions well, but also enables the prediction of adsorption isotherms that were not included in the training set of the model.

In the present study, we have have transferred that modeling approach to the description of the adsorption of BSA. To obtain a basis for this work, we have systematically studied the influence of sodium chloride, sodium sulfate, ammonium chloride, and ammonium sulfate for ionic strengths between 0 mM and 3000 mM and of the pH value on the adsorption of BSA on Toyopearl MX-Trp-650M in equilibrium adsorption experiments. The pH values were chosen as follows: pH 4.0, where BSA carries a positive net charge but is, in contrast to smaller pH values [18], still stable in the F-conformation in solution; pH 4.7, where BSA carries approximately zero net charge and is present in the N-conformation; and pH 7.0, where BSA is still in the N-conformation but carries a negative net charge. The temperature was always 25 °C. The adsorption data was used for developing and training a model that describes the adsorption of BSA as a function of the studied parameters. The model can for example be used for the conceptual process design of MMC processes.

2 Materials and methods

2.1 Materials

Bovine serum albumin (BSA, $M = 66.4$ kDa) with a purity over 98% was obtained from Sigma-Aldrich. The mixed-mode resin Toyopearl MX-Trp-650M, whose tryptophan ligands possess weak carboxyl cation exchange as well as indole hydrophobic functional groups, was obtained from Tosoh Bioscience. All salts used for buffer preparations were of analytical grade: citric acid ($C_6H_8O_7$) and trisodium citrate dihydrate ($Na_3C_6H_5O_7 \cdot 2H_2O$) were used for the preparation of 25 mM sodium citrate buffers with pH 4.0 or 4.7; sodiumdihydrogen phosphate dihydrate ($NaH_2PO_4 \cdot 2H_2O$) and disodiumhydrogen phosphate dihydrate ($Na_2HPO_4 \cdot 2H_2O$) were used for the preparation of a 25 mM sodium phosphate buffer with pH 7.0. As additional salts, sodium chloride (NaCl), sodium sulfate (Na_2SO_4), ammonium chloride (NH_4Cl), and ammonium sulfate ($(NH_4)_2SO_4$) were used. 1 N sodium hydroxide (NaOH) and 1 N hydrochloric acid (HCl) were used for the adjustment of the pH value of the buffer solutions. Trisodium citrate dihydrate was obtained from Sigma-Aldrich and ammonium chloride from Bernd Kraft. All other chemicals used for buffer preparations were obtained from Carl-Roth. The ultrapure water used as solvent for all buffers was produced with a Milli-Q water purification system from Merck Millipore.

2.2 Batch adsorption experiments

Batch adsorption experiments were performed with a fully automated liquid handling station Freedom EVO 200 from Tecan. The adsorption equilibrium measurements were carried out as described by [28], so that in the following only a brief overview is given. For the experiments at pH 4.0 and 4.7, a 25 mM sodium citrate buffer with the respective pH value was used. Each studied salt (sodium chloride, sodium sulfate, ammonium chloride, and ammonium sulfate) was added gravimetrically to the respective buffer yielding different ionic strengths I up to 3000 mM. For the experiments at pH 7.0, a 25 mM sodium phosphate buffer was used; at this pH value, again all four salts were studied but only at two ionic strengths: $I = 250$ mM and $I = 3000$ mM. In each case, the pH value of the resulting salt solution was adjusted to the desired value with 1 N sodium hydroxide or 1 N hydrochloric acid after dissolving the salt in the respective buffer. Subsequently, BSA stock solutions were prepared by adding BSA gravimetrically to the respective final salt solutions and dissolving it.

All experiments were carried out in 96-well Riplate plates from Ritter. In each well, 500 µl BSA solution and 50.9 µl of the mixed-mode adsorbent were dispensed for the equilibrium adsorption experiments. After the equilibration time (6 h at 25 °C), the BSA concentration in the liquid phase was measured by UV absorption at 280 nm. BSA-free solutions were measured as blank values for each batch adsorption experiment, i.e., for each studied salt, ionic strength, and pH value. We adopt here the estimate of the relative uncertainty of the equilibrium loading of the resin of 10% from [34], who carried out similar experiments with the same equipment, though for very small loadings lager uncertainties may occur.

2.3 Data processing

The adsorption data obtained from the batch experiments were correlated with the semi-empirical approach of [35] and [36]:

$$c_{\mathrm{BSA}}^{(m)} = \frac{q_{\mathrm{BSA}}^{(m)}}{K^{\mathrm{ads}}} \cdot \exp\left[\beta \cdot \sqrt{q_{\mathrm{BSA}}^{(m)}/q_0^{(m)}} \cdot \exp\frac{-\gamma}{\sqrt{q_{\mathrm{BSA}}^{(m)}/q_0^{(m)}}}\right] \tag{1}$$

where c_{BSA} is the free BSA concentration in solution and q_{BSA} denotes the BSA loading of the resin. The adsorption equilibrium constant K^{ads} describes the initial slope of the correlated adsorption isotherm (at $c_{\mathrm{BSA}} \to 0$), while the lumped fitting parameters β and γ, which were made dimensionless by introducing $q_0^{(m)} = 1$ mg/ml, characterize the overall isotherm shape. Equation (1) was used for correlating the data from the batch adsorption experiments only, i.e., to fit the individual equilibrium isotherms, which was subsequently the basis for developing a predictive model as described in the following. Generally, any other mathematical function that is flexible enough for describing the experimental data could have been used instead of Eq. (1) without substantially affecting the modeling results.

All data processing and modeling steps were carried out with MATLAB. As the four studied salts (sodium chloride, sodium sulfate, ammonium chloride, and ammonium sulfate) possess different ion valences, results are discussed in terms of ionic strength I, calculated using ion concentrations c_i, in the following:

$$I = \frac{1}{2}\sum_i c_i z_i^2 = \text{const.} \tag{2}$$

where z_i denotes the charge number of the respective ion i. The small concentration of buffer salts ($c = 25$ mM) present in all solutions was neglected in this calculation.

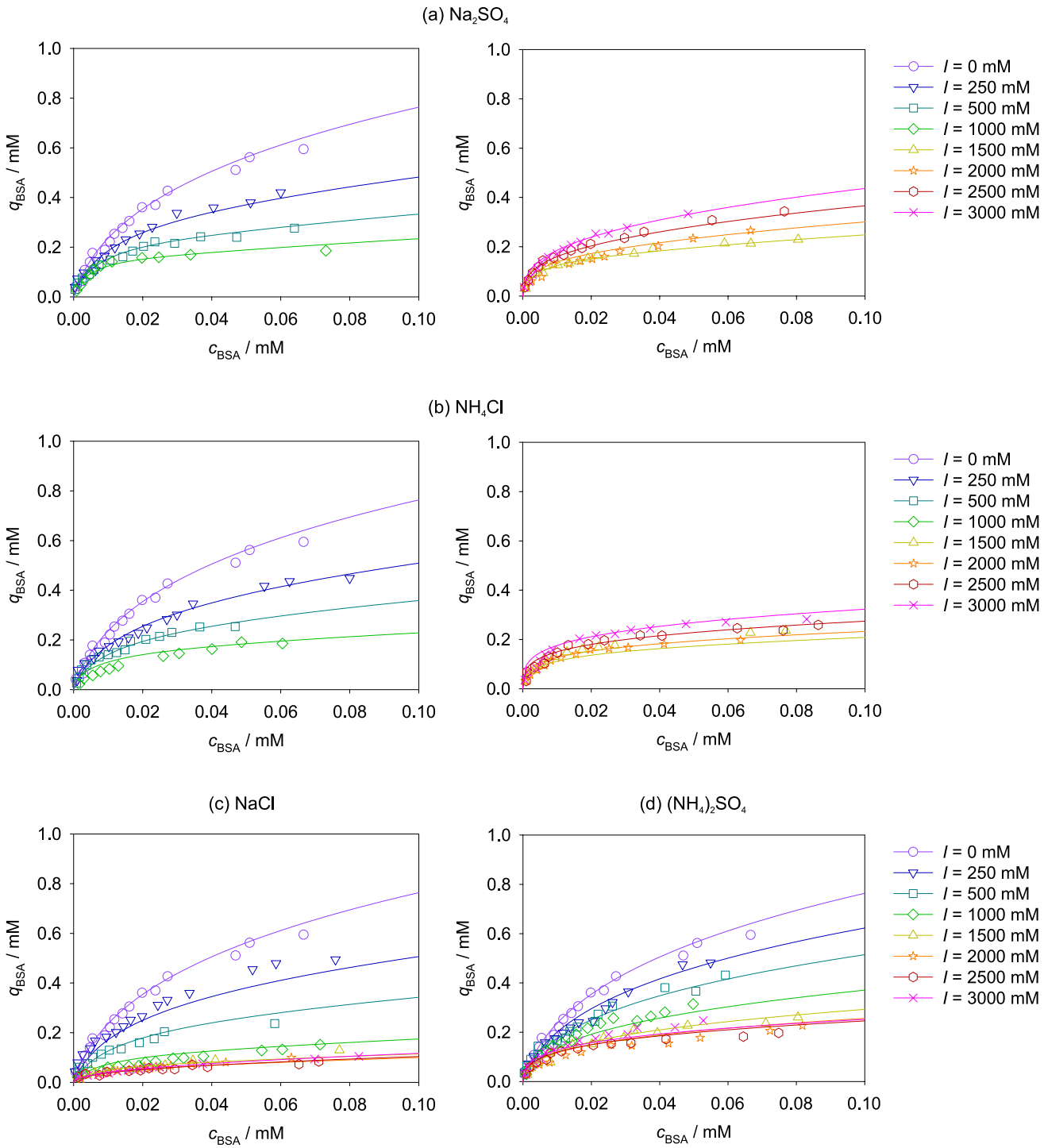

Fig. 1 Equilibrium adsorption isotherms of BSA on Toyopearl MX-Trp-650M at pH 4.0 and 25 °C for four salts at different ionic strengths *I*. Symbols: experimental data; lines: model

3 Results and discussion

3.1 Experimental adsorption isotherms

In Fig. 1, the results of the batch adsorption experiments with the four studied salts at pH 4.0 are shown. Data for sodium sulfate (a) and ammonium chloride (b) are displayed in separate diagrams for low and high ionic strengths for improved clarity. The symbols denote the experimental data whereas the lines show the results of the model developed in this work, which is described in detail below, cf. Sections 3.2 - 3.3. For the sake of completeness, the corresponding correlations of the individual experimental isotherms at pH 4.0 with Eq. (1) are shown together with the experimental data in Figure S.1 in the Supporting Information.

In general, the adsorption of BSA on the mixed-mode resin can be divided into two regions depending on the predominant adsorption mechanism: the region at rather low ionic strengths, where adsorption is mainly caused by ionic interactions, will be called IEC region in the following, and the region at rather high ionic strengths, where hydrophobic interactions are dominant, will subsequently be called HIC region. The results show that the protein adsorption is stronger in the IEC region than in the HIC region, which indicates, as expected, that the ionic interactions are stronger than the hydrophobic interactions.

In the IEC region up to approximately $I = 1000$ mM, the BSA loading decreases with increasing ionic strength for all studied salts at pH 4.0, where BSA carries a positive net charge. The highest BSA loading is found at $I = 0$ mM, i.e., for the salt-free solution. The decrease of the BSA loading with increasing ionic strength is mainly caused by the shielding effect of the ions, which hamper the ionic interactions between BSA and the cation exchange ligands, and by the cations competing with the BSA molecules for the adsorption sites.

At ionic strengths above about $I = 1000$ mM the situation changes. Depending on the type of salt, the BSA loading increases with increasing ionic strength (sodium sulfate and ammonium chloride, cf. Figure 1(a),(b), respectively) or remains rather constant (sodium chloride and ammonium sulfate, cf. Figure 1(c),(d), respectively). This observation is explained by an increasing salting-out effect, which enhances hydrophobic interactions between BSA and the HIC sites of the resin with increasing ionic strength and at some point outweighs the decreasing adsorption on the IEC sites.

In Fig. 2, the experimental adsorption data of BSA at pH 4.7 as well as the model results for the presence of the four studied salts are shown. The corresponding correlations of the individual isotherms with Eq. (1) at pH 4.7 are shown together with the experimental data in Figure S.2 in the Supporting Information.

The influence of the ionic strength on the BSA adsorption at pH 4.7 is similar to the one found at pH 4.0. At pH 4.7, the adsorption decreases with increasing ionic strength in the IEC region and increases with increasing ionic strength in the HIC region for all studied salts as well. However, the adsorption in the IEC region (with the exception of the adsorption at $I = 0$ mM) is at a similar level as in the HIC region. At $I = 0$ mM, i.e., without the addition of salts, the IEP is at approx. pH 4.7 [13]; with increasing ionic strength, the IEP of BSA slightly decreases [13], so that BSA is slightly negatively charged at pH 4.7 and $I > 0$ mM, leading to little ionic interactions there. In contrast to pH 4.0, at pH 4.7 for all salts a similar but rather small increase of the adsorption with increasing ionic strength is found in the HIC region.

The results for the adsorption of BSA at pH 7.0 in the presence of the four studied salts are shown in Figure S.3 in the Supporting Information. For both ionic strengths studied at pH 7.0, namely, $I = 250$ mM and $I = 3000$ mM, the adsorption of BSA is only weak. Especially in the IEC region at $I = 250$ mM, there is almost no BSA adsorption, except for sodium chloride. Due to the negative net charge of both the BSA molecules and the cation exchange ligands of the mixed-mode resin at pH 7.0, repulsive ionic forces are strongly predominant. The slightly higher adsorption of BSA in the presence of sodium chloride compared to the other salts at pH 7.0 and $I = 250$ mM can be attributed to its rather strong shielding effect of the repulsive negative surface charges of BSA and the IEC ligands due to the small sodium and chloride ions. The adsorption of BSA at $I = 3000$ mM is very similar for all salts and higher than at $I = 250$ mM for all salts (except for sodium chloride), which can be explained by the increasing salting-out effect in the HIC region.

Since the negative net charge of BSA at pH 7.0 is in general unfavorable for an adsorption on a mixed-mode resin that contains IEC ligands, no experiments at other ionic strengths than $I = 250$ mM and $I = 3000$ mM were carried out. Firstly, the results for these conditions are less relevant for practical applications and secondly, the rather low level of adsorption leads to large experimental uncertainties of the adsorption data. Therefore, the results obtained at pH 7.0 were not included in the model development and fitting process described below, cf. Sections 3.2 - 3.3.

To further study the influence of the salts on the different interaction mechanisms of the mixed-mode resin, a comparison of the BSA loading of the studied mixed-mode resin Toyopearl MX-Trp-650M and the single-mode HIC resin PPG-600M [30] is given in Figure S.4 in the Supporting Information for all studied salts. At $I = 1500$ mM, i.e., in the transition region (between the IEC and the HIC region)

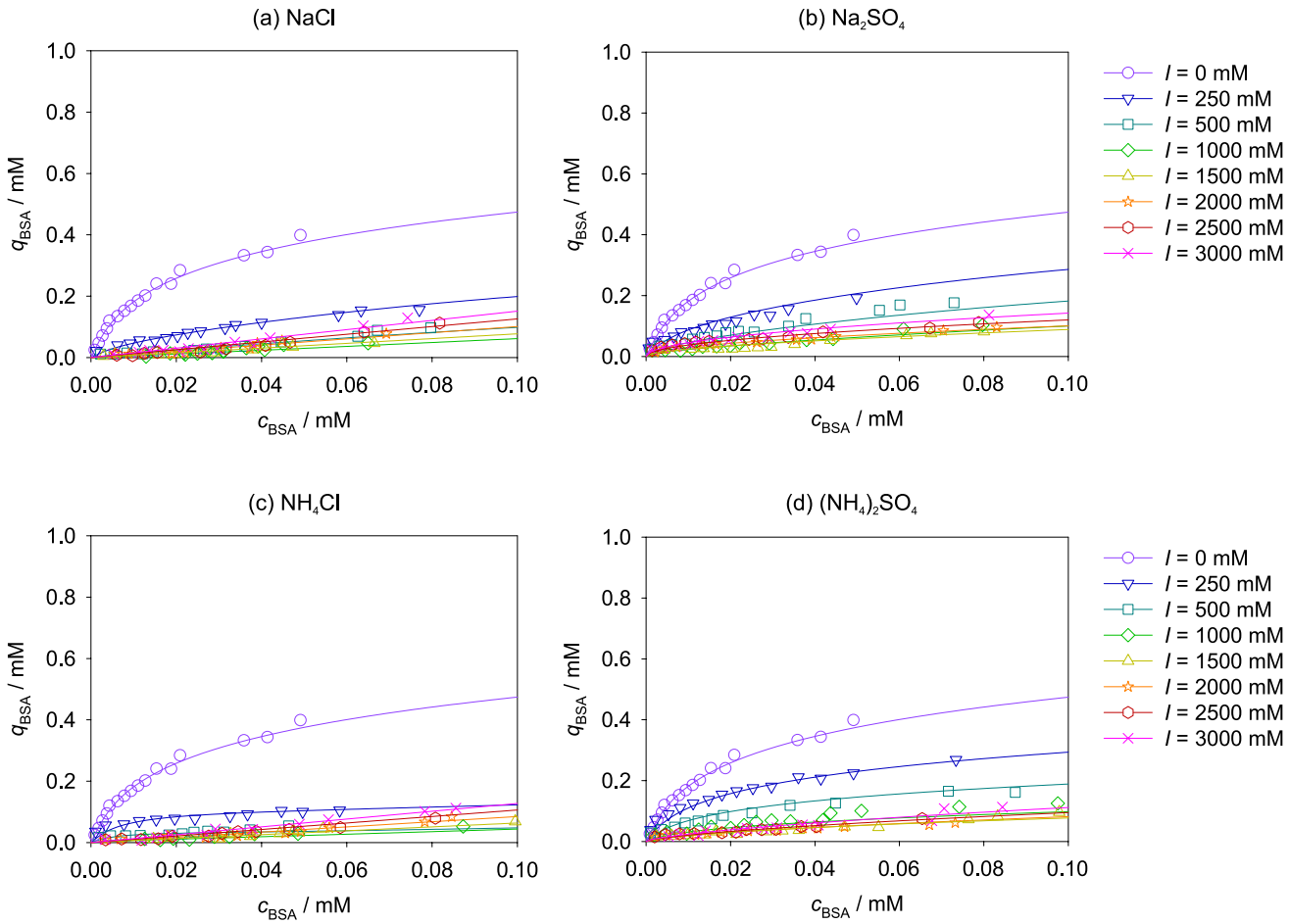

Fig. 2 Equilibrium adsorption isotherms of BSA on Toyopearl MX-Trp-650M at pH 4.7 and 25 °C for four salts at different ionic strengths *I*. Symbols: experimental data; lines: model

of the mixed-mode resin, the type of salt influences whether the adsorption on the mixed-mode or the single-mode resin is higher. Salts containing sulfate ions (especially ammonium sulfate) lead to higher BSA loadings of the mixed-mode resin indicating strong ionic interactions for these two salts, while salts containing chloride ions (especially sodium chloride) lead to lower loadings on the mixed-mode than on the single-mode resin, which indicates a dominance of the hydrophobic interactions and, hence, weaker ionic interactions for these two salts.

For assessing the influence of the pH value in more detail, Fig. 3 shows the adsorption isotherms of BSA for solutions containing sodium sulfate and ammonium chloride, respectively, for two ionic strengths that were chosen as examples ($I = 250$ mM and $I = 3000$ mM) for all studied pH values (pH 4.0, 4.7, and 7.0). The two salts were chosen here as they exhibit the strongest influence on the adsorption in the HIC region, cf. Figures 1 and 2, and the ionic strengths were chosen to show results for the two interaction regions: at $I = 250$ mM adsorption is mainly caused by the cation exchange mechanism and at $I = 3000$ mM by hydrophobic interactions. Figure 3 also includes the results of the developed model for pH 4.0 and 4.7 (lines), whereas at pH 7.0 the experimental results are shown together with the corresponding individual correlations, cf. Equation (1). The respective results of the batch adsorption experiments with the two other studied salts, namely, sodium chloride and ammonium sulfate, are shown in Figure S.5 in the Supporting Information.

At $I = 250$ mM, the adsorption decreases significantly with increasing pH value, which agrees well with the expectation. Adsorption is dominated by ionic interactions at this ionic strength. At pH 4.0, where BSA carries a positive net charge, the highest loadings are observed for all salts, cf. also Figure S.5 in the Supporting Information; at pH 4.7, i.e., close to the IEP of BSA, adsorption is significantly smaller for all salts; at pH 7.0, adsorption is weak due to the negative net charge of both BSA and the ionic ligands of the mixed-mode resin. The pH value can in general not only have an influence on the net charge of the protein, but also on the

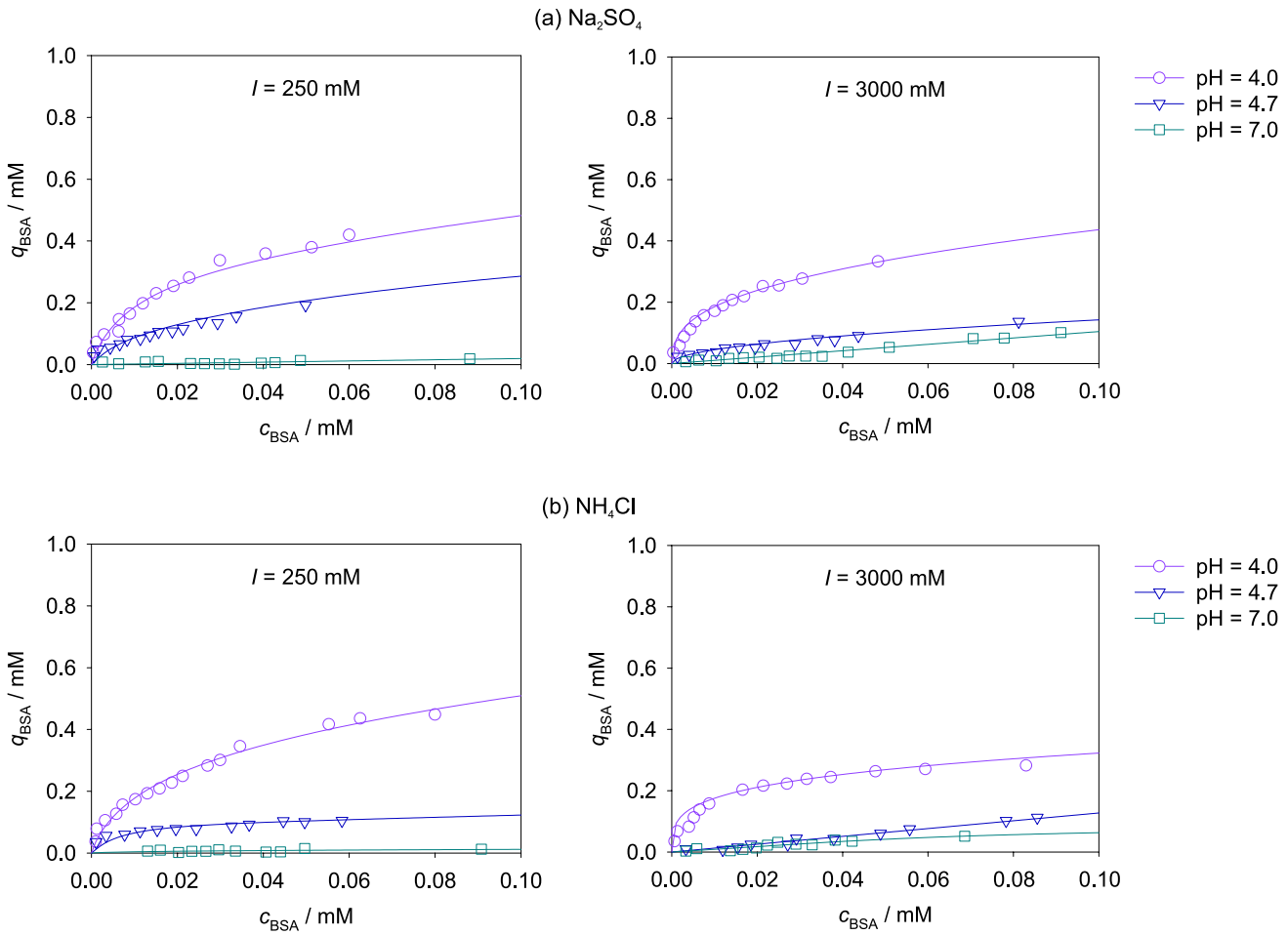

Fig. 3 Equilibrium adsorption isotherms of BSA on Toyopearl MX-Trp-650M at pH 4.0, 4.7, and 7.0 and 25 °C for (**a**) sodium sulfate and (**b**) ammonium chloride. Symbols: experimental data; lines: model for pH 4.0 and 4.7, and individual correlations for pH 7.0, cf. Equation (1)

dissociation equilibrium of the acid cation exchange ligands of the mixed-mode resin and therefore on the net charge of the resin. An experimental investigation of the dissociation of the used resin is out of the scope of the present work, so that only qualitative statements are made here. An increasing pH value enhances the dissociation, which, however, seems to be outweighed by the dependence of the protein's net charge on the pH value leading to the higher adsorption at pH 4.0 than at 4.7. At pH 7.0, the higher degree of dissociation of the ionic ligands additionally strengthens the repulsion between protein molecules and ligands.

At $I = 3000$ mM, i.e., in the HIC region, the highest adsorption is also found at pH 4.0 for all salts, cf. also Figure S.5 in the Supporting Information. The expanded F-BSA present at pH 4.0 exhibits a larger surface area that is accessible for hydrophobic interactions with the HIC ligands compared to the more globular N-BSA present at pH 4.7 and 7.0 [18], which in turn leads to a stronger adsorption at pH 4.0 compared to the other pH values. The adsorption of BSA at pH 4.7 and 7.0 is similar for all studied salts, i.e., there is no significant difference in the adsorption for these two pH values here. This supports the assumption that the conformation of BSA in solution is the main influencing factor for the adsorption at high ionic strengths. However, the repulsing net charges of the protein and the resin at pH 7.0 are potentially slightly weakening the adsorption even at high ionic strengths, i.e., where many ions for shielding the ionic repulsion are present, which is why slightly higher adsorption is found at pH 4.7 than at 7.0 for all studied salts. Also here the results for sodium chloride differ from those of the other salts: the low adsorption at high ionic strengths of sodium chloride at pH 4.0 can be explained by a low salting-out effect of the chaotropic salt sodium chloride according to the Hofmeister series [37].

3.2 Model development

The semi-empirical function of Oberholzer and Lenhoff, cf. Eq. (1), is not suitable for generalizing over conditions or

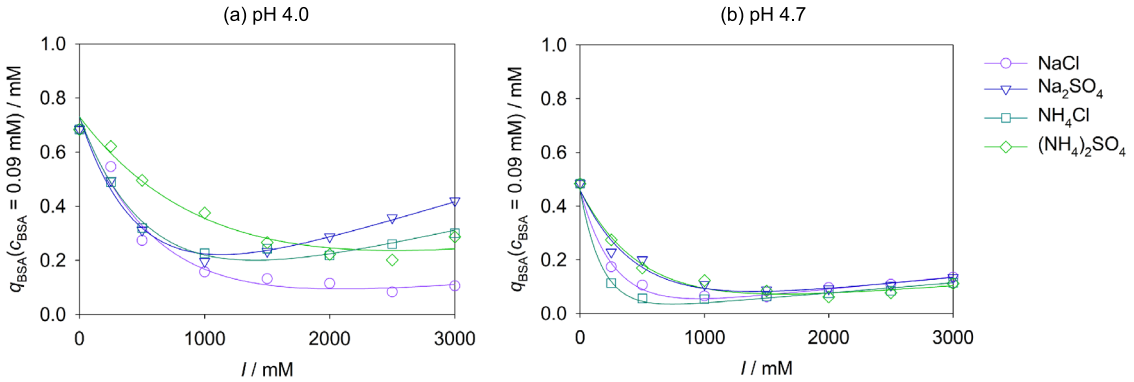

Fig. 4 BSA loading q_{BSA} of Toyopearl MX-Trp-650M at a liquid phase concentration $c_{BSA} = 0.09$ mM at 25 °C for all studied salts as a function of the ionic strength I at (**a**) pH 4.0 and (**b**) pH 4.7. Symbols: experimental results (correlated with Eq. (1)); lines: model, cf. Eq. (3)

even to predict adsorption isotherms for unstudied conditions, since the fitting parameters of the individual correlations do not show any dependence on the studied process parameters, cf. Tables S.1 - S.3 in the Supporting Information. Therefore, in the following, we describe the development of a new model of the adsorption of BSA on the mixed-mode resin Toyopearl MX-Trp-650M, which describes the influence of the ionic strength of the four studied salts for different pH values. The model is based on an approach introduced for describing the adsorption of lysozyme on Toyopearl MX-Trp-650M from our previous work [27, 28]. In this prior work and in contrast to the present work, no significant increase of the protein (i.e., lysozyme) adsorption with increasing ionic strength in the HIC region was found, which is why we have extended the approach in the present work to improve the description of the BSA loading in the HIC region at high ionic strengths.

3.2.1 Dependence of the loading on the ionic strength

In a first step, the individual adsorption isotherms for pH 4.0 and 4.7 fitted with Eq. (1) were discretized. Therefore, the BSA loading was calculated from the individual correlations for a defined concentration of BSA in the liquid phase c_{BSA}. This was done in increments of 0.01 mM starting from $c_{BSA} = 0.01$ mM up to $c_{BSA} = 0.1$ mM. As an example, Fig. 4 shows results for $c_{BSA} = 0.09$ mM; this concentration is also indicated in the presentation of the individual correlations in Figures S.1 and S.2 in the Supporting Information by vertical dashed lines, but the respective diagrams for other concentrations of BSA are very similar, cf. Figure S.6 in the Supporting Information.

For all salts and both pH values, an exponential decay of the adsorption with increasing ionic strength is observed in the IEC region (up to approximately $I = 1000$ mM). Hence, the influence of the addition of salt on the adsorption is proportional to the amount of salt already present in solution in this region. This behaviour was already observed for the adsorption of lysozyme on the same mixed-mode resin at pH 5.0, 6.0, and 7.0 [27, 28]. Moreover, results from other studies, e.g., for the adsorption of BSA and plasma-derived human serum albumin (pHSA) on a mixed-mode resin support this observation [23, 24].

At pH 4.0, adsorption is especially strong in the IEC region if ammonium sulfate is present, while it is lower and rather similar for the other studied salts at the same ionic strength. We can explain this by considering the size of the ions: the large ammonium and sulfate ions exhibit, compared to the smaller ions, a rather weak shielding effect leading to the smallest exponential decay found for this salt. The presence of rather strong ionic interactions if ammonium sulfate is present in comparison to the other studied salts (at the same ionic strength) was also observed when comparing the adsorption on the mixed-mode resin to the one on the single-mode HIC resin as discussed for Figure S.4 (a) in the Supporting Information.

At pH 4.7 and low ionic strengths, the adsorption is stronger if sulfate ions are present than this is the case for chloride ions. This implies that the type of anion is more decisive than the type of cation. The greater exponential decay of the BSA loading with increasing ionic strength at low ionic strengths for the addition of sodium chloride in comparison to ammonium sulfate also agrees with reports in the literature [23].

In the HIC region above about $I = 1000$ mM, the adsorption increases at some point with increasing ionic strength for all four salts and both pH values (though the extent of the increase strongly differs), which demonstrates the salt-tolerant nature of the mixed-mode resin. However, the loading of BSA at the highest studied ionic strength, i.e., $I = 3000$ mM, is still lower than the adsorption measured at $I = 0$ mM, i.e., in the IEC region, for all four salts, as the ionic interactions are generally stronger than the hydrophobic interactions.

At pH 4.0, the linear increase with increasing ionic strength is especially noticeable with the addition of sodium sulfate and ammonium chloride. In contrast, the increase is much weaker (and the adsorption remains almost constant) upon the addition of the other two salts, namely, sodium chloride and ammonium sulfate. The combination of a small and a large ion, as it is the case for sodium sulfate and ammonium chloride, seems to be particularly attractive for a strong adsorption of F-BSA.

In contrast, at pH 4.7, the adsorption only slightly increases with increasing ionic strength for $I > 1000$ mM for all four studied salts. Furthermore, in this region, no significant influence of the type of salt is observed. Hence, the smaller accessible surface area of N-BSA seems to limit the amount of hydrophobic interactions regardless of the additional salt present in solution.

For modeling the dependence of the BSA loading q_{BSA} at a constant BSA concentration in the liquid phase c_{BSA} on the ionic strength I for a given salt S, cf. Figures 4 and S.6 in the Supporting Information, a superposition of two functions was chosen: one that describes the exponential decay with increasing ionic strength (which dominates in the IEC region and is similar to the one used in our previous work [27, 28]), and a second one that describes the linear increase with ionic strength (which dominates in the HIC region):

$$\frac{q_{\mathrm{BSA}}(c_{\mathrm{BSA}} = \text{const.})}{\mathrm{mM}} = k_0^{(\mathrm{IEC})} \cdot \exp\left(-k_S^{(\mathrm{IEC})} \cdot \frac{I}{1000\ \mathrm{mM}}\right) + k_S^{(\mathrm{HIC})} \cdot \frac{I}{1000\ \mathrm{mM}} \tag{3}$$

where $k_0^{(\mathrm{IEC})}$ describes the adsorption in salt-free solution (at $I = 0$ mM, $q_{\mathrm{BSA}}(c_{\mathrm{BSA}} = \text{const.})$ equals $k_0^{(\mathrm{IEC})}$), whereas $k_S^{(\mathrm{IEC})}$ and $k_S^{(\mathrm{HIC})}$ are salt-specific parameters that describe the influence of the respective salt on the cation exchange adsorption mechanism and on the hydrophobic adsorption mechanism, respectively.

The resulting model fits with Eq. (3) are in excellent agreement with the data from the individual adsorption isotherms as shown in Figs. 4 and S.6 in the Supporting Information. The description of the BSA loading correctly represents the exponential decay at low ionic strengths and the linear increase at high ionic strengths for all four studied salts and both pH values.

3.2.2 Dependence of model parameters on the BSA concentration

To obtain a model that can describe complete adsorption isotherms, the dependence of the parameters of Eq. (3), namely, $k_0^{(\mathrm{IEC})}$, $k_S^{(\mathrm{IEC})}$, and $k_S^{(\mathrm{HIC})}$, on the BSA concentration in the liquid phase needs to be considered, this dependence is shown in Fig. 5 for the four studied salts at pH 4.0 and 4.7; respectively. Simple trends are observed, which support the model assumptions.

The dependence of the parameter for salt-free adsorption $k_0^{(\mathrm{IEC})}$ on the BSA concentration describes the equilibrium adsorption isotherm in the salt-free solution. As expected, values for $k_0^{(\mathrm{IEC})}$ for pH 4.0 are always higher than for pH 4.7. The dependence of $k_0^{(\mathrm{IEC})}$ on c_{BSA} was obtained in the same way as in our previous work [27, 28], using the semi-empirical function of Oberholzer and Lenhoff, which was already used in Eq. (1) for correlating the individual isotherms and reads here as shown in Eq. (4):

$$\frac{c_{\mathrm{BSA}}}{\mathrm{mM}} = \frac{k_0^{(\mathrm{IEC})}}{a_0^{(\mathrm{IEC})}} \cdot \exp\left[b_0^{(\mathrm{IEC})} \cdot \sqrt{k_0^{(\mathrm{IEC})}} \cdot \exp\frac{-d_0^{(\mathrm{IEC})}}{\sqrt{k_0^{(\mathrm{IEC})}}}\right] \tag{4}$$

where the parameters $a_0^{(\mathrm{IEC})}$, $b_0^{(\mathrm{IEC})}$, and $d_0^{(\mathrm{IEC})}$ correspond to the parameters K^{ads}, β, and γ from Eq. (1), respectively, but molar concentrations are used instead of mass concentrations here.

The dependence of the salt-specific parameter for low ionic strengths $k_S^{(\mathrm{IEC})}$ on the BSA concentration is different for the various salts, especially at pH 4.7. However, at both pH values, the parameter for ammonium sulfate shows the lowest absolute values, which matches the expectations; the large ammonium and sulfate ions exhibit the weakest shielding effects. The dependence of $k_S^{(\mathrm{IEC})}$ on c_{BSA}, describing how strong a specific salt S affects the adsorption in the exponential decay of the BSA loading, was modeled with a function adopted from our previous work [27, 28]:

$$k_S^{(\mathrm{IEC})} = a_S^{(\mathrm{IEC})} - b_S^{(\mathrm{IEC})} + b_S^{(\mathrm{IEC})} \cdot \exp\left(-d_S^{(\mathrm{IEC})} \cdot \frac{c_{\mathrm{BSA}}}{\mathrm{mM}}\right) \tag{5}$$

where the salt-dependent parameters $a_S^{(\mathrm{IEC})}$, $b_S^{(\mathrm{IEC})}$, and $d_S^{(\mathrm{IEC})}$ describe the influence of the salts on the IEC mechanism of the adsorption.

The salt-specific parameter for high ionic strengths $k_S^{(\mathrm{HIC})}$ clearly increases with the BSA concentration for all studied salts. At pH 4.0, a distinct order regarding the type of salt can be determined. For sodium sulfate and ammonium chloride the highest values for $k_S^{(\mathrm{HIC})}$ are obtained, leading to the strongest increase of adsorption at high ionic strengths, cf. also Fig. 4. The results for $k_S^{(\mathrm{HIC})}$ at pH 4.7 for the different salts have similar values, which is in line with the finding that the type of salt has no significant influence on the adsorption here, cf. Figure 4(b). For modeling $k_S^{(\mathrm{HIC})}$ as a function of c_{BSA}, a new model equation was introduced:

$$k_S^{(\mathrm{HIC})} = a_S^{(\mathrm{HIC})} \cdot \left(\frac{c_{\mathrm{BSA}}}{\mathrm{mM}}\right)^{b_S^{(\mathrm{HIC})}} \tag{6}$$

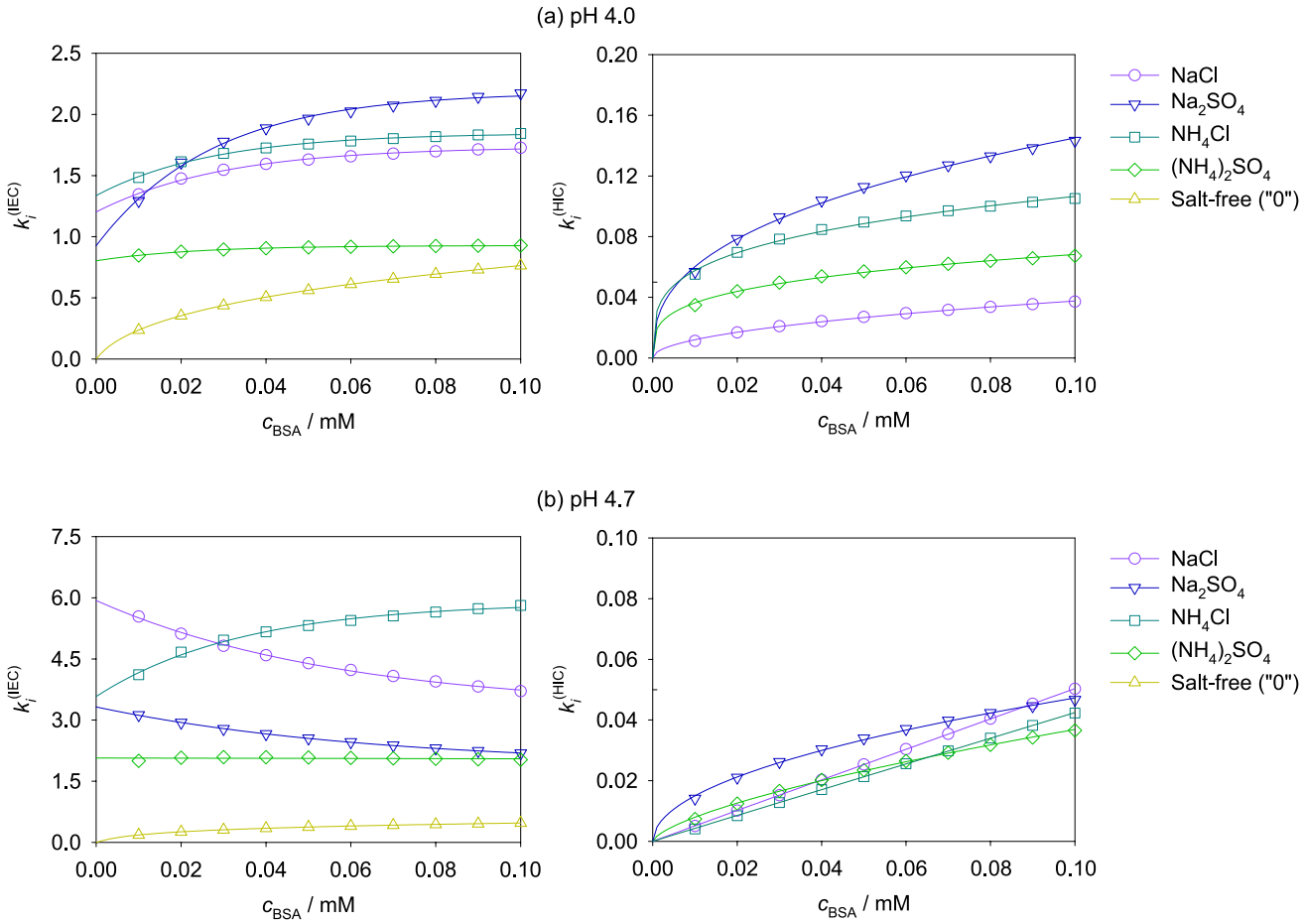

Fig. 5 Parameters $k_0^{(IEC)}$, $k_S^{(IEC)}$, and $k_S^{(HIC)}$ of Eq. (3) for describing the dependence of the BSA loading on the ionic strength plotted over the BSA concentration in the liquid phase c_{BSA} for all studied salts at (**a**) pH 4.0 and (**b**) pH 4.7. Symbols: results at constant c_{BSA} from Eq. (3); lines: model of the concentration-dependence of the parameters, cf. Eqs. (4), (5), or (6). Left panel: parameters describing IEC interactions; right panel: parameters describing HIC interactions

where the salt-dependent parameters $a_S^{(HIC)}$ and $b_S^{(HIC)}$ describe the influence of the salts on the HIC mechanism of the adsorption.

As shown by the lines in Fig. 5, Eqs. (4–6) allow an excellent description of the dependence of the parameters $k_0^{(IEC)}$, $k_S^{(IEC)}$, and $k_S^{(HIC)}$ on c_{BSA}. The resulting model parameters a_i, b_i, and d_i are summarized in Table 1.

3.3 Prediction of equilibrium adsorption isotherms

By inserting Eqs. (4–6) in Eq. (3), a final model equation for the description of equilibrium adsorption isotherms of BSA on Toyopearl MX-Trp-650M at 25 °C is obtained. The model can be used for predicting adsorption isotherms for all studied salts at any ionic strength. There are two sets of parameters, one for pH 4.0 and one for pH 4.7, see Table 1. We have refrained from reporting a model for the dependence of the parameters on the pH value to enable predictions at other pH values, as we have only two supporting points, between which we could only interpolate linearly. Furthermore, we know from our data at pH 7.0 using such a linear function is over-simplistic and does not capture the complex physics of the pH dependence (involving, e.g., conformation changes of BSA) adequately. The agreement of the model results with the experimental data is very good as shown in Figs. 1 and 2. The model correctly describes the influence of the different salts and the ionic strength for both considered pH values.

The proposed model can be used for the prediction of adsorption isotherms within the trained condition range, e.g., at other ionic strengths, as applied for the comparison of MMC and HIC data in Figure S.4 (a) in the Supporting

Table 1 Model parameters of Eqs. (4–6) for the prediction of entire equilibrium adsorption isotherms of BSA on Toyopearl MX-Trp-650M at 25 °C at pH 4.0 and 4.7

pH	Mechanism	Salt i	a_i	b_i	d_i
4.0	IEC	None ("0")	42.421	3.636	0.539
		NaCl	1.202	−0.534	33.464
		Na_2SO_4	0.926	−1.258	36.571
		NH_4Cl	1.337	−0.512	36.130
		$(NH_4)_2SO_4$	0.803	−0.125	43.608
	HIC	NaCl	0.117	0.495	-
		Na_2SO_4	0.349	0.382	-
		NH_4Cl	0.197	0.267	-
		$(NH_4)_2SO_4$	0.128	0.274	-
4.7	IEC	None ("0")	29.008	10.807	0.974
		NaCl	5.935	2.660	17.465
		Na_2SO_4	3.322	1.438	15.380
		NH_4Cl	3.581	−2.308	29.131
		$(NH_4)_2SO_4$	2.069	7.063	0.027
	HIC	NaCl	0.497	0.994	-
		Na_2SO_4	0.149	0.498	-
		NH_4Cl	0.421	0.996	-
		$(NH_4)_2SO_4$	0.171	0.667	-

Information. Also extrapolations to conditions outside but not too far from the training conditions might be possible, cf. also [27] where extrapolations for a similar type of model were analyzed.

3.4 Comparison of BSA and lysozyme loadings

It is interesting to compare the results of BSA obtained in the present work with those obtained for lysozyme in our previous work [27, 28], as both studies were carried out with the same resin, the same salts, and for similar pH values. Results of the comparison are shown in Fig. 6, where the protein loading is reported as a function of the ionic strength for pH 4.7 for all studied salts. The comparison is carried out for a fixed protein concentration in the solutions $c_P = 0.09$ mM, which was already used previously, cf. Figure 4. The results for BSA stem from the model developed in this work, cf. Eqs. (3–6), those for lysozyme were obtained by extrapolations with the model developed in our prior work [27, 28].

Figure 6 reveals important differences between the adsorption of both proteins. In the largest part of the studied range of the ionic strength, the adsorption of lysozyme is much stronger than that of BSA at the studied pH value. This is related to the higher net charge of lysozyme at the studied pH value, which leads to stronger ionic interactions between lysozyme and the mixed-mode resin compared to BSA. Similar results can be found at pH 7.0 as well, cf. Figure S.7 in the Supporting Information.

Only at very high ionic strengths, i.e., in the HIC region, an inverse trend is observed for most of the salts, see also the enlarged representation in Fig. 6 (right): the adsorption of BSA is stronger than that of lysozyme, albeit on an overall low level. As observed previously, the BSA loading increases with increasing ionic strength, which can not be observed for lysozyme, cf. [27] and [28], indicating only little hydrophobic interactions of lysozyme with the mixed-mode resin. Lysozyme is a rather "hard" protein [38, 39], which retains its secondary structure also during adsorption [40], while BSA is a rather "soft" protein [38, 39]. The more flexible BSA can therefore change its confirmation, allowing stronger hydrophobic interactions with the mixed-mode resin due to the varying solvent-accessible surface areas. We thus speculate that at even higher ionic strengths than 3000 mM, an even stronger adsorption of BSA can be expected for all salts and pH values.

The shown comparison of the loading of BSA and lysozyme can be considered as an example that demonstrates the usefulness of the presented modeling approach, e.g., for the conceptual design of protein separation processes.

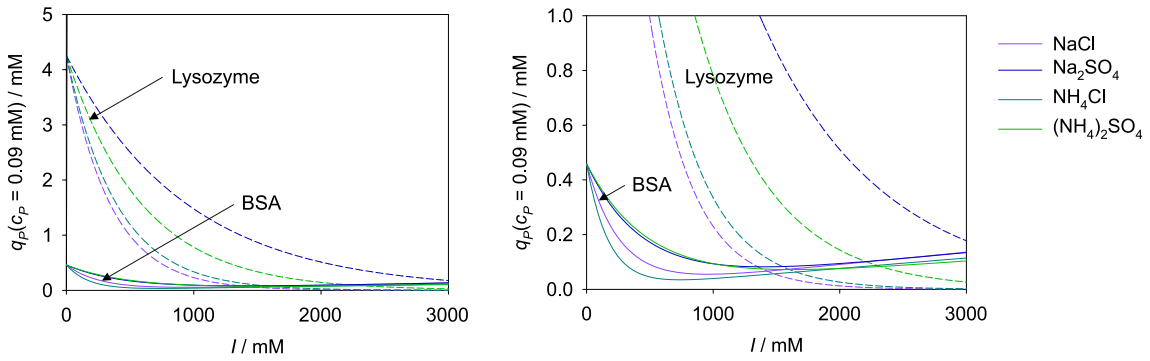

Fig. 6 Comparison of BSA and lysozyme loading of Toyopearl MX-Trp-650M at $c_P = 0.09$ mM (P ={BSA,lysozyme}) at pH 4.7 and 25 °C for all studied salts as a function of the ionic strength I. Solid lines: BSA loading, cf. Eqs. (3–6); dashed lines: lysozyme loading, cf. [27] and [28]. The right panel shows a zoomed-in representation of the left panel and was included for improved clarity

Model interpretations always dependent on protein and resin properties. Salts can have various influences on the adsorption of proteins. E.g., BSA has been observed to follow the Hofmeister series while lysozyme was described to follow the Hofmeister series only at high ionic strengths [41-44] However, the results of this work as well as our previous study on lysozyme with the same resin [27] did not show an adsorption behavior of any of the two proteins that can be explained by the Hofmeister series. Nevertheless, the presented modeling approach is generic so that is can be applied to different combinations of proteins and resins and, thus, could be used for finding optimized process conditions with a reduced experimental effort.

The fact that a similar type of model could be used for the successful description of adsorption isotherms of lysozyme in our previous work [27, 28] indicates that this modeling approach is also applicable for other systems, namely, other combinations of proteins and mixed-mode resins.

4 Conclusion

In the present work, a systematic experimental study of the adsorption of BSA on the mixed-mode resin Toyopearl MX-Trp-650M was carried out at 25 °C. The influence of different salts (sodium chloride, sodium sulfate, ammonium chloride, and ammonium sulfate), the ionic strength (0 to 3000 mM), and the pH value (4.0, 4.7, and 7.0) was studied. At pH 4.0 and 4.7, where BSA carries a positive net charge or almost no net charge, respectively, the adsorption of BSA can be divided into two regions for all studied salts. In the IEC region up to approximately $I = 1000$ mM, the adsorption is dominated by ionic interactions between the protein and the cation exchange ligands or the resin, and the loading decreases exponentially with increasing ionic strength. Ions shield both, the negatively charged cation exchange ligands as well as the charged amino acids on the BSA surface. Particularly effective shielding effects were found for salts containing small ions (sodium and chloride). In the HIC region at higher ionic strengths, the adsorption is mainly caused by hydrophobic interactions and increases nearly linearly with increasing ionic strength, which is due to the salting-out effect of the salts present in solution. The strongest salting-out effects were observed for sodium sulfate and ammonium chloride at pH 4.0.

In all cases, the BSA loading decreases with increasing pH value, which is mainly caused by the dependence of the net charge of BSA on the pH value. The strongest adsorption was found at pH 4.0 and the lowest at pH 7.0, where adsorption was very low due to the negative net charge of both the BSA and the cation exchange ligands of the resin. The strongest hydrophobic interactions were found at pH 4.0, which can be explained by the expanded F-BSA conformation, in which BSA is present at this condition, whereas the more globular N-BSA conformation is present at pH 4.7 and 7.0. In future work, also the properties of the proteins and pure resins should be studied, particularly the dissociation equilibria and the related surface charges as a function of pH value and ionic strength of different salts.

Furthermore, we have developed a mathematical model of the adsorption of BSA on Toyopearl MX-Trp-650M. The model describes the influence of the salt type, the ionic strength, and the pH value on the BSA loading; equilibrium adsorption isotherms that are predicted with the model are in very good agreement with the experimental data. Since the model can predict equilibrium adsorption isotherms for a wide range of relevant process parameters, it is a valuable tool for the simulation, conceptual design, and optimization of separation processes of proteins with mixed-mode chromatography. The modeling approach is generic and can be transferred to other systems, e.g., proteins and resins.

Supplementary Information The online version of this article contains supplementary material available https://doi.org/10.1007/s10450-023-00384-0.

Acknowledgements FJ gratefully acknowledges financial support from the Ministry of Science and Health of the Federal State of Rhineland-Palatinate.

Funding Open Access funding enabled and organized by Projekt DEAL. FJ gratefully acknowledges financial support from the Ministry of Science and Health of the Federal State of Rhineland-Palatinate.

Declarations

Conflict of interest There are no competing interests to declare.

References

1. Kaleas, K.A., Schmelzer, C.H., Pizarro, S.A.: Industrial case study: Evaluation of a mixed-mode resin for selective capture of a human growth factor recombinantly expressed in e. coli. J. Chromatogr. A **1217**(2), 235–242 (2010). https://doi.org/10.1016/j.chroma.2009.07.023
2. Zhang, K., Liu, X.: Mixed-mode chromatography in pharmaceutical and biopharmaceutical applications. J. Pharm. Biomed. Anal. **128**, 73–88 (2016). https://doi.org/10.1016/j.jpba.2016.05.007

3. Brochier, V.B., Schapman, A., Santambien, P., et al.: Fast purification process optimization using mixed-mode chromatography sorbents in pre-packed mini-columns. J. Chromatogr. A **1177**(2), 226–233 (2008). https://doi.org/10.1016/j.chroma.2007.08.086
4. Gao, D., Lin, D.Q., Yao, S.J.: Measurement and correlation of protein adsorption with mixed-mode adsorbents taking into account the influences of salt concentration and pH. J. Chem. Eng. Data **51**(4), 1205–1211 (2006). https://doi.org/10.1021/je050528p
5. Gao, D., Lin, D.Q., Yao, S.J.: Protein adsorption kinetics of mixed-mode adsorbent with benzylamine as functional ligand. Chem. Eng. Sci. **61**(22), 7260–7268 (2006). https://doi.org/10.1016/j.ces.2006.07.013
6. Lu, M.H., Lin, D.Q., Wu, Y.C., et al.: Separation of nattokinase fromBacillus subtilis fermentation broth by expanded bed adsorption with mixed-mode adsorbent. Biotechnol. Bioprocess Eng. **10**(2), 128–135 (2005). https://doi.org/10.1007/bf02932582
7. Chung, W.K., Hou, Y., Holstein, M., et al.: Investigation of protein binding affinity in multimodal chromatographic systems using a homologous protein library. J. Chromatogr. A **1217**(2), 191–198 (2010). https://doi.org/10.1016/j.chroma.2009.08.005
8. Holstein, M.A., Nikfetrat, A.A., Gage, M., et al.: Improving selectivity in multimodal chromatography using controlled pH gradient elution. J. Chromatogr. A **1233**, 152–155 (2012). https://doi.org/10.1016/j.chroma.2012.01.074
9. Lan, Q., Bassi, A.S., Zhu, J.X.J., et al.: A modified langmuir model for the prediction of the effects of ionic strength on the equilibrium characteristics of protein adsorption onto ion exchange/affinity adsorbents. Chem. Eng. J. **81**(1–3), 179–186 (2001). https://doi.org/10.1016/s1385-8947(00)00197-2
10. Xia, F., Nagrath, D., Cramer, S.M.: Effect of pH changes on water release values in hydrophobic interaction chromatographic systems. J. Chromatogr. A **1079**(1–2), 229–235 (2005). https://doi.org/10.1016/j.chroma.2005.04.005
11. Lienqueo, M.E., Mahn, A., Salgado, J.C., et al.: Current insights on protein behaviour in hydrophobic interaction chromatography. J. Chromatogr. B **849**(1–2), 53–68 (2007). https://doi.org/10.1016/j.jchromb.2006.11.019
12. Grönberg, A.: Ion exchange chromatography Biopharmaceutical Processing, pp. 379–399. Elsevier, Netherlands (2018). https://doi.org/10.1016/b978-0-08-100623-8.00018-9
13. Salis, A., Bostroem, M., Medda, L., et al.: Measurements and theoretical interpretation of points of zero charge/potential of BSA protein. Langmuir **27**(18), 11,597-11,604 (2012). https://doi.org/10.1021/la2024605
14. Barbosa, L.R., Ortore, M.G., Spinozzi, F., et al.: The importance of protein-protein interactions on the pH-induced conformational changes of bovine serum albumin: A small-angle x-ray scattering study. Biophys. J. **98**(1), 147–157 (2010). https://doi.org/10.1016/j.bpj.2009.09.056
15. Seeber, S., White, J., Hem, S.: Predicting the adsorption of proteins by aluminium-containing adjuvants. Vaccine **9**(3), 201–203 (1991). https://doi.org/10.1016/0264-410x(91)90154-x
16. Peters, T.: The albumin molecule All About Albumin. Elsevier, Netherlands (1995). https://doi.org/10.1016/b978-012552110-9/50004-0
17. Carter, D.C., Ho, J.X.: Structure of serum albumin. Lipoproteins, Apolipoproteins, and Lipases., pp. 153–203. Elsevier, Netherlands (1994). https://doi.org/10.1016/s0065-3233(08)60640-3
18. Baler, K., Martin, O.A., Carignano, M.A., et al.: Electrostatic unfolding and interactions of albumin driven by pH changes: a molecular dynamics study. J. Phys. Chem. B **118**(4), 921–930 (2014). https://doi.org/10.1021/jp409936v
19. Gao, D., Yao, S.J., Lin, D.Q.: Preparation and adsorption behavior of a cellulose-based, mixed-mode adsorbent with a benzylamine ligand for expanded bed applications. J. Appl. Polym. Sc. **107**(1), 674–682 (2007). https://doi.org/10.1002/app.26958
20. Gomes, P.F., Loureiro, J.M., Rodrigues, A.E.: Adsorption equilibrium and kinetics of immunoglobulin g on a mixed-mode adsorbent in batch and packed bed configuration. J. Chromatogr. A **1524**, 143–152 (2017). https://doi.org/10.1016/j.chroma.2017.10.003
21. Gomes, P.F., Loureiro, J.M., Rodrigues, A.E.: Adsorption of human serum albumin (HSA) on a mixed-mode adsorbent: equilibrium and kinetics. Adsorption **23**(4), 491–505 (2017). https://doi.org/10.1007/s10450-017-9861-x
22. Zhu, M., Carta, G.: Protein adsorption equilibrium and kinetics in multimodal cation exchange resins. Adsorption **22**(2), 165–179 (2015). https://doi.org/10.1007/s10450-015-9735-z
23. Chang, Y.K., Chou, S.Y., Liu, J.L., et al.: Characterization of BSA adsorption on mixed mode adsorbent. Biochem. Eng. J. **35**(1), 56–65 (2007). https://doi.org/10.1016/j.bej.2006.12.026
24. Wu, Q.C., Lin, D.Q., Shi, W., et al.: A mixed-mode resin with tryptamine ligand for human serum albumin separation. J. Chromatogr. A **1431**, 145–153 (2016). https://doi.org/10.1016/j.chroma.2015.12.066
25. Ghose, S., Hubbard, B., Cramer, S.M.: Protein interactions in hydrophobic charge induction chromatography (hcic). Biotechnol. Prog. **21**(2), 498–508 (2005). https://doi.org/10.1021/bp049712+
26. Nfor, B.K., Noverraz, M., Chilamkurthi, S., et al.: High-throughput isotherm determination and thermodynamic modeling of protein adsorption on mixed mode adsorbents. J. Chromatogr. A **1217**(44), 6829–6850 (2010). https://doi.org/10.1016/j.chroma.2010.07.069
27. Kreusser, J., Jirasek, F., Hasse, H.: Influence of pH value and salts on the adsorption of lysozyme in mixed-mode chromatography. Eng. Life Sci. **21**(11), 753–768 (2021). https://doi.org/10.1002/elsc.202100058
28. Kreusser, J., Jirasek, F., Hasse, H.: Influence of salts on the adsorption of lysozyme on a mixed-mode resin. Adsorpt. Sci. Technol. **2021**, 1–11 (2021). https://doi.org/10.1155/2021/6681348
29. Galeotti, N., Hackemann, E., Jirasek, F., et al.: Prediction of the elution profiles of proteins in mixed salt systems in hydrophobic interaction chromatography. Sep. Purifi. Technol. **233**(116), 006 (2020). https://doi.org/10.1016/j.seppur.2019.116006
30. Hackemann, E., Hasse, H.: Influence of mixed electrolytes and pH on adsorption of bovine serum albumin in hydrophobic interaction chromatography. J. Chromatogr. A **1521**, 73–79 (2017). https://doi.org/10.1016/j.chroma.2017.09.024
31. Hackemann, E., Hasse, H.: Mathematical modeling of adsorption isotherms in mixed salt systems in hydrophobic interaction chromatography. Biotechnol. Prog. **34**(5), 1251–1260 (2018). https://doi.org/10.1002/btpr.2683
32. Hackemann, E., Werner, A., Hasse, H.: Influence of mixed electrolytes on the adsorption of lysozyme, PEG, and PEGylated lysozyme on a hydrophobic interaction chromatography resin. Biotechnol. Progr. **33**(4), 1104–1115 (2017). https://doi.org/10.1002/btpr.2474
33. Werner, A., Hasse, H.: Experimental study and modeling of the influence of mixed electrolytes on adsorption of macromolecules on a hydrophobic resin. J. Chromatogr. A **1315**, 135–144 (2013). https://doi.org/10.1016/j.chroma.2013.09.071
34. Werner, A., Blaschke, T., Hasse, H.: Microcaloric study of the adsorption of pegylated lysozyme and peg on a mildly hydrophobic resin: influence of ammonium-sulfate. Langmuir **28**, 11,376-11,383 (2012). https://doi.org/10.1021/la302239e
35. Chang, C., Lenhoff, A.M.: Comparison of protein adsorption isotherms and uptake rates in preparative cation-exchange materials. J. Chromatogr. A **827**(2), 281–293 (1998). https://doi.org/10.1016/s0021-9673(98)00796-1

36. Oberholzer, M.R., Lenhoff, A.M.: Protein adsorption isotherms through colloidal energetics. Langmuir **15**(11), 3905–3914 (1999). https://doi.org/10.1021/la981199k
37. Hofmeister, F.: Zur lehre von der wirkung der salze. Archiv für Exp. Pathol. und Pharm. **24**(4–5), 247–260 (1888). https://doi.org/10.1007/bf01918191
38. Norde, W., Anusiem, A.C.: Adsorption, desorption and re-adsorption of proteins on solid surfaces. Colloids Surf. **66**(1), 73–80 (1992). https://doi.org/10.1016/0166-6622(92)80122-i
39. Norde, W., Giacomelli, C.E.: Conformational changes in proteins at interfaces: From solution to the interface, and back. Macromol. Symp. **145**(1), 125–136 (1999). https://doi.org/10.1002/masy.19991450114
40. Mücksch, C., Urbassek, H.M.: Forced desorption of bovine serum albumin and lysozyme from graphite: Insights from molecular dynamics simulation. J. Phys. Chem. B **120**(32), 7889–7895 (2016). https://doi.org/10.1021/acs.jpcb.6b05234
41. Boström, M., Parsons, D.F., Salis, A., et al.: Possible origin of the inverse and direct hofmeister series for lysozyme at low and high salt concentrations. Langmuir **27**(15), 9504–9511 (2011). https://doi.org/10.1021/la202023r
42. Paterová, J., Rembert, K.B., Heyda, J., et al.: Reversal of the hofmeister series: Specific ion effects on peptides. J. Phys. Chem. B **117**(27), 8150–8158 (2013). https://doi.org/10.1021/jp405683s
43. Schwierz, N., Horinek, D., Sivan, U., et al.: Reversed hofmeister series—the rule rather than the exception. Curr. Opi. Colloid Interface Sci. **23**, 10–18 (2016). https://doi.org/10.1016/j.cocis.2016.04.003
44. Zhang, Y., Cremer, P.S.: The inverse and direct hofmeister series for lysozyme. Proc. Natl. Acad. Sci. **106**(36), 15249–15253 (2009). https://doi.org/10.1073/pnas.0907616106